Pretreatment with a γ-Secretase Inhibitor Prevents Tumor-like Overgrowth in Human iPSC-Derived Transplants for Spinal Cord Injury

Toshiki Okubo,[1,2] Akio Iwanami,[1] Jun Kohyama,[2] Go Itakura,[2] Soya Kawabata,[1] Yuichiro Nishiyama,[1] Keiko Sugai,[1] Masahiro Ozaki,[1,2] Tsuyoshi Iida,[1,2] Kohei Matsubayashi,[1,2] Morio Matsumoto,[1] Masaya Nakamura,[1,*] and Hideyuki Okano[2,*]

[1]Department of Orthopaedic Surgery
[2]Department of Physiology
Keio University School of Medicine, 35 Shinanomachi, Shinjuku-ku, Tokyo 160-8582, Japan
*Correspondence: masa@a8.keio.jp (M.N.), hidokano@a2.keio.jp (H.O.)
http://dx.doi.org/10.1016/j.stemcr.2016.08.015

SUMMARY

Neural stem/progenitor cells (NS/PCs) derived from human induced pluripotent stem cells (hiPSCs) are considered to be a promising cell source for cell-based interventions that target CNS disorders. We previously reported that transplanting certain hiPSC-NS/PCs in the spinal cord results in tumor-like overgrowth of hiPSC-NS/PCs and subsequent deterioration of motor function. Remnant immature cells should be removed or induced into more mature cell types to avoid adverse effects of hiPSC-NS/PC transplantation. Because Notch signaling plays a role in maintaining NS/PCs, we evaluated the effects of γ-secretase inhibitor (GSI) and found that pretreating hiPSC-NS/PCs with GSI promoted neuronal differentiation and maturation in vitro, and GSI pretreatment also reduced the overgrowth of transplanted hiPSC-NS/PCs and inhibited the deterioration of motor function in vivo. These results indicate that pretreatment with hiPSC-NS/PCs decreases the proliferative capacity of transplanted hiPSC-NS/PCs, triggers neuronal commitment, and improves the safety of hiPSC-based approaches in regenerative medicine.

INTRODUCTION

Embryonic stem cells and induced pluripotent stem cells (iPSCs) can differentiate into neural stem/progenitor cells (NS/PCs), which can subsequently be induced in vitro to differentiate into three neural lineages: neurons, astrocytes, and oligodendrocytes (Falk et al., 2012; Miura et al., 2009; Okada et al., 2004). Furthermore, accumulating evidence suggests that NS/PCs represent a promising cell source for regenerative medicine targeting CNS disorders (Cummings et al., 2005; Hofstetter et al., 2005; Iwanami et al., 2005; Kumagai et al., 2009; Nori et al., 2011; Okada et al., 2005, 2008; Ogawa et al., 2002; Salazar et al., 2010; Yasuda et al., 2011). Our previous reports have shown that transplantation of NS/PCs derived from human induced pluripotent stem cells (hiPSC-NS/PCs) promotes motor function recovery in non-obese diabetic-severe combined immune-deficient (NOD-SCID) mice and non-human primates with spinal cord injury (SCI) (Fujimoto et al., 2012; Kobayashi et al., 2012; Nori et al., 2011; Okano et al., 2013; Tsuji et al., 2010). However, transplanting certain hiPSC-NS/PCs, such as clone 253G1 (generated through a process of retroviral transfection), results in tumor-like overgrowth and deterioration of motor function during long-term observations (Nori et al., 2015), and transplanting clone 836B3 (episomal plasmid vectors) in an SCI animal model yielded similar results during long-term observations (our unpublished data). Moreover, these tumors consisted of undifferentiated human-specific Nestin+ cells.
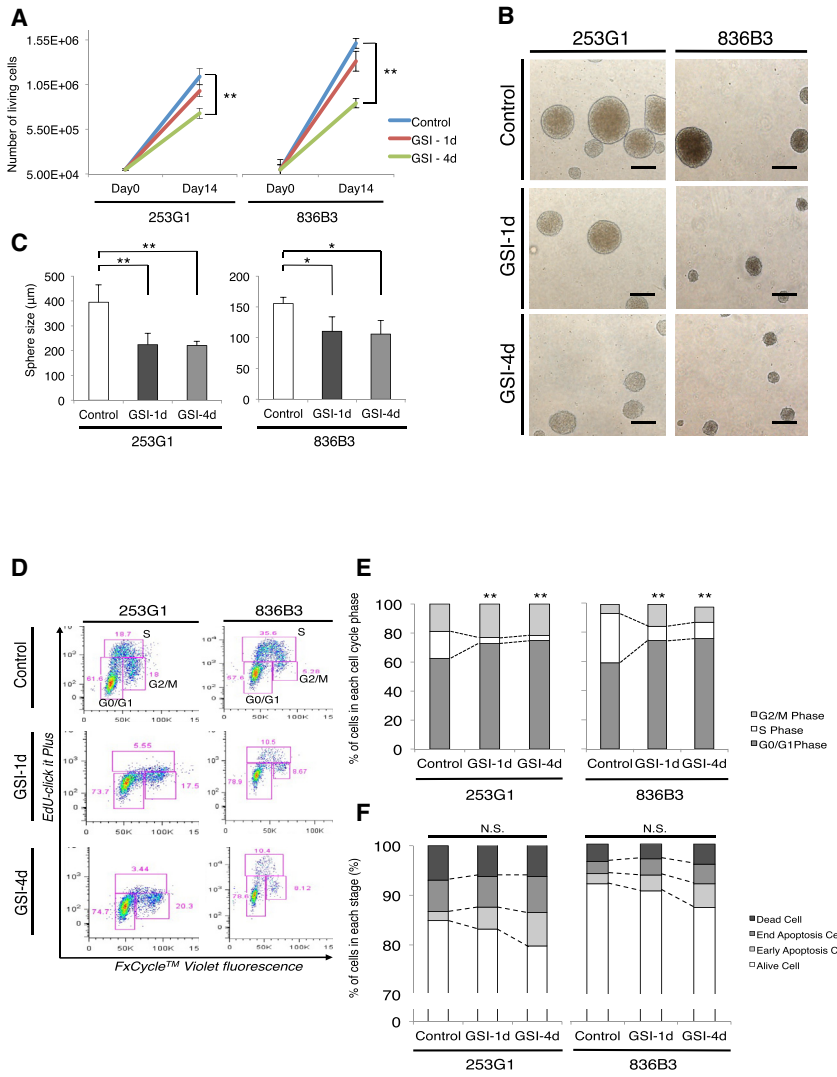
The safety of measures for preventing tumor-like overgrowth is of great importance in clinical applications of iPSC-based transplantation therapy for SCI. Remnant immature NS/PCs must be removed or induced to differentiate into more mature cell types, which may avoid tumor-like overgrowth following transplantation. Notch signaling controls the induction of NS/PCs, and inhibition of this signaling with a γ-secretase inhibitor (GSI) induces the NS/PCs to develop into a more mature state with limited proliferation in vitro (Crawford and Roelink, 2007; Nelson et al., 2007). Treatment of iPSC-derived dopaminergic progenitor cells with GSIs prior to transplantation into the normal mid-striatum is known to control the growth of a potentially proliferative cell population in vivo (Ogura et al., 2013).

The purpose of the present study was to elucidate the effects of a GSI on the proliferation and differentiation of tumorigenic hiPSC-NS/PCs in vitro, assess the effects of GSI pretreatment on the hiPSC-NS/PCs in vivo, and determine whether animal models of SCI exhibit recovered motor functions and an absence of tumor-like overgrowth following transplantation of the pretreated cells.

RESULTS

Treatment with the GSI Suppressed the Proliferation of hiPSC-NS/PCs

We performed differentiation and proliferation assays using hiPSC-NS/PCs in vitro. After treating the cells with

or without GSI, aggregated hiPSC-NS/PCs were dissociated into single cells and the living cells were counted. In the GSI-4d group (hiPSC-NS/PCs cultured in vitro with GSI for 4 days), the number of living cells was significantly decreased compared with that of the other groups (253G1: control 1.14×10^6 cells, GSI-1d [hiPSC-NS/PCs cultured in vitro with GSI for 1 day] 9.80×10^5 cells, GSI-4d 7.28×10^5 cells; 836B3: control 1.51×10^6 cells, GSI-1d 1.31×10^6 cells, GSI-4d, 8.42×10^5 cells; Figure 1A). Next, the size of the sphere was measured by microscopy after treatment with or without GSI. In the control group, the size of the sphere was significantly increased compared with that of both GSI groups (253G1: control 394.7 ± 69.5 μm, GSI-1d 224.1 ± 46.1 μm, GSI-4d 220.4 ± 17.3 μm; 836B3: control 155.2 ± 10.7 μm, GSI-1d 110.4 ± 23.6 μm, GSI-4d 105.9 ± 21.8 μm; Figures 2B and 2C).

In the cell-cycle analyses, representative dot plots of the flow cytometry data revealed a reduced S-phase population among the GSI-treated hiPSC-NS/PCs (Figure 1D). Compared with the control group, the proportion of cells in G_0/G_1 phase was significantly increased (253G1: control 62.6% ± 2.7%, GSI-1d 72.8% ± 1.1%, GSI-4d 74.8% ± 1.8%; 836B3: control 58.9% ± 1.3%, GSI-1d 74.4% ± 2.3%, GSI-4d 75.7% ± 2.9%). The proportion of cells in the S phase was significantly decreased in both GSI groups (253G1: control 18.6% ± 0.8%, GSI-1d 4.1% ± 0.2%, GSI-4d 3.6% ± 0.1%; 836B3: control 33.8% ± 0.9%, GSI-1d 9.6% ± 0.6%, GSI-4d 11.2% ± 1.2%; Figure 1E). According to the annexin V/7-AAD apoptosis assay, the proportion of early apoptotic cells was slightly increased in both GSI groups compared with the control group, although significant differences were not observed among these groups (253G1: control 2.01% ± 0.2%,

GSI-1d 4.1% ± 0.3%, GSI-4d 5.5% ± 0.4%; 836B3: control 2.0% ± 0.5%, GSI-1d 3.1% ± 0.3%, GSI-4d 4.7% ± 0.5%). These results suggest that GSI treatment could induce the differentiation of undifferentiated hiPSC-NS/PCs.

GSI Induced Differentiation into More Mature Neuronal Cell Types with Limited Cell Proliferation

Next, we assessed the effects of GSI on the neuronal differentiation and maturation of hiPSC-NS/PCs. In both GSI groups, the proportion of Ki-67$^+$ (a cell proliferation marker) and Nestin$^+$ (a neural stem cell marker) cells was also significantly decreased compared with that of the control group (Ki-67$^+$ cells: 253G1—control 45.2% ± 1.4%, GSI-1d 30.7% ± 2.2%, GSI-4d 28.1% ± 0.8%; 836B3—control 34.0% ± 2.7%, GSI-1d 16.7% ± 1.9%, GSI-4d 13.0% ± 1.7%; Nestin$^+$ cells: 253G1—control 60.8% ± 1.9%, GSI-1d 36.6% ± 1.2%, GSI-4d 30.9% ± 1.4%; 836B3—control 43.6% ± 2.1%, GSI-1d 34.1% ± 0.5%, GSI-4d 23.6% ± 1.1%; Figures 2A–2D), whereas the proportion of βIII-tubulin$^+$ neurons was significantly increased (253G1: control 70.9% ± 2.3%, GSI-1d 94.7% ± 3.1%, GSI-4d 94.3% ± 2.4%; 836B3: control 47.6% ± 4.8%, GSI-1d 86.0% ± 4.9%, GSI-4d 86.7% ± 5.0%). The proportion of GFAP$^+$ astrocytes and CNPase$^+$ (2′,3′-cyclic-nucleotide 3′-phosphodiesterase) oligodendrocytes was not significantly different among the three groups (Figures 2E–2H). Microelectrode array (MEA) analyses indicated that neuronal maturation was significantly enhanced in both GSI groups compared with the control group (Figure 2J).

Gene Expression Profiles of hiPSC-NS/PCs after the GSI Treatment

DNA microarray analyses were performed on the hiPSC-NS/PCs that were treated with or without GSI to evaluate the gene expression profiles of the cells. Following the GSI treatment, 61 genes were downregulated (downregulation: 97 genes in the GSI-1d group, 274 genes in the GSI-4d group; Figure 3A) and 53 genes were upregulated (upregulation: 58 genes in the GSI-1d group, 147 genes in the GSI-4d group; Figure 3B) in 253G1 hiPSC-NS/PCs. In 836B3 hiPSC-NS/PCs, 26 genes were downregulated (downregulation: 49 genes in the GSI-1d group, 63 genes in the GSI-4d group; Figure 3C) and seven genes were upregulated (upregulation: eight genes in the GSI-1d group, 77 genes in the GSI-4d group; Figure 3D). Functional association analyses showed that the expression of cell-cycle-related genes and more mature neuronal marker-related genes increased by >2-fold in both GSI groups compared with the control group. Significant increases in the levels of p53-dependent genes, such as CDKN1C and GADD45G, and more neuronal maturation-dependent genes, such as NEUROG1, NEUROD1, and ASCL1, were detected (Figures 3E and 3F).

Gene Ontology (GO) analyses identified a number of neuronal differentiation- and maturation-associated terms, such as "neuron differentiation," "neuron development," "developmental maturation," "regulation of cell cycle," and "neuron projection development," in the GSI-treated hiPSC-NS/PCs (Tables S1 and S2).

We performed RT-PCR to validate these findings, which showed that the expression of representative Notch signaling target genes, such as HES5 and NOTCH1, was nearly abolished by pretreatment with GSI (Figure S1A). In addition, the expression of early neural marker genes, such as SOX2 and PAX6, was also downregulated in both GSI groups. The expression of mature neuronal marker genes, such as NEUROG2, ASCL1, and NEUROD1 (but not glial markers, such as GFAP and OLIG2), was upregulated, as expected, given the downregulated expression of pluripotency/self-renewal markers, such as NANOG, LIN28, OCT4, and NESTIN (Figures S1B–S1D).

Next, we confirmed the role of Notch signaling in the specification of hiPSC-NS/PCs by comparing the qRT-PCR analyses for each cell line after treatment with or without GSI. The data were presented as expression levels relative to the 836B3 hiPSC-NS/PCs. The expression of Notch signaling-related genes, such as JAGGED1, NOTCH1, and PSEN1, was significantly upregulated in the 253G1 hiPSC-NS/PCs, which seemed to indicate that Notch signaling was increased in the 253G1 hiPSC-NS/PCs compared with the 836B3 hiPSC-NS/PCs. Under these activation conditions, the expression of the HES5, HEYL, HSPB1, ID2, ID4, NESTIN, OCT3/4, VCAM1, and NANOG genes were particularly downregulated in the GSI-treated groups compared with the control group. Additionally for each cell line, the GSI treatment resulted in a decrease in the expression of the target genes of Notch signaling, such as JAGGED1 and NRARP (Figures S2A and S2B).

Previous transcriptome analyses by our group revealed the altered expression of genes involved in epithelial-mesenchymal transition (EMT), which plays roles in tumor invasion and progression, following the transplantation of 253G1 hiPSC-NS/PCs (Nori et al., 2015). The expression of EMT-related genes, such as SNAIL1, SNAIL2, TWIST1, and TWIST2, was downregulated in the GSI-treated group compared with the control group (Figure 3G).

Long-Term Observations after Transplantation of Tumorigenesis-/Overgrowth-Prone hiPSC-NS/PCs that Had Been Pretreated with GSI

Next, we examined the long-term effects of GSI pretreatment on hiPSC-NS/PCs that had been transplanted into SCI model mice in vivo and focused on the potency of the GSI treatment in preventing the tumor-like
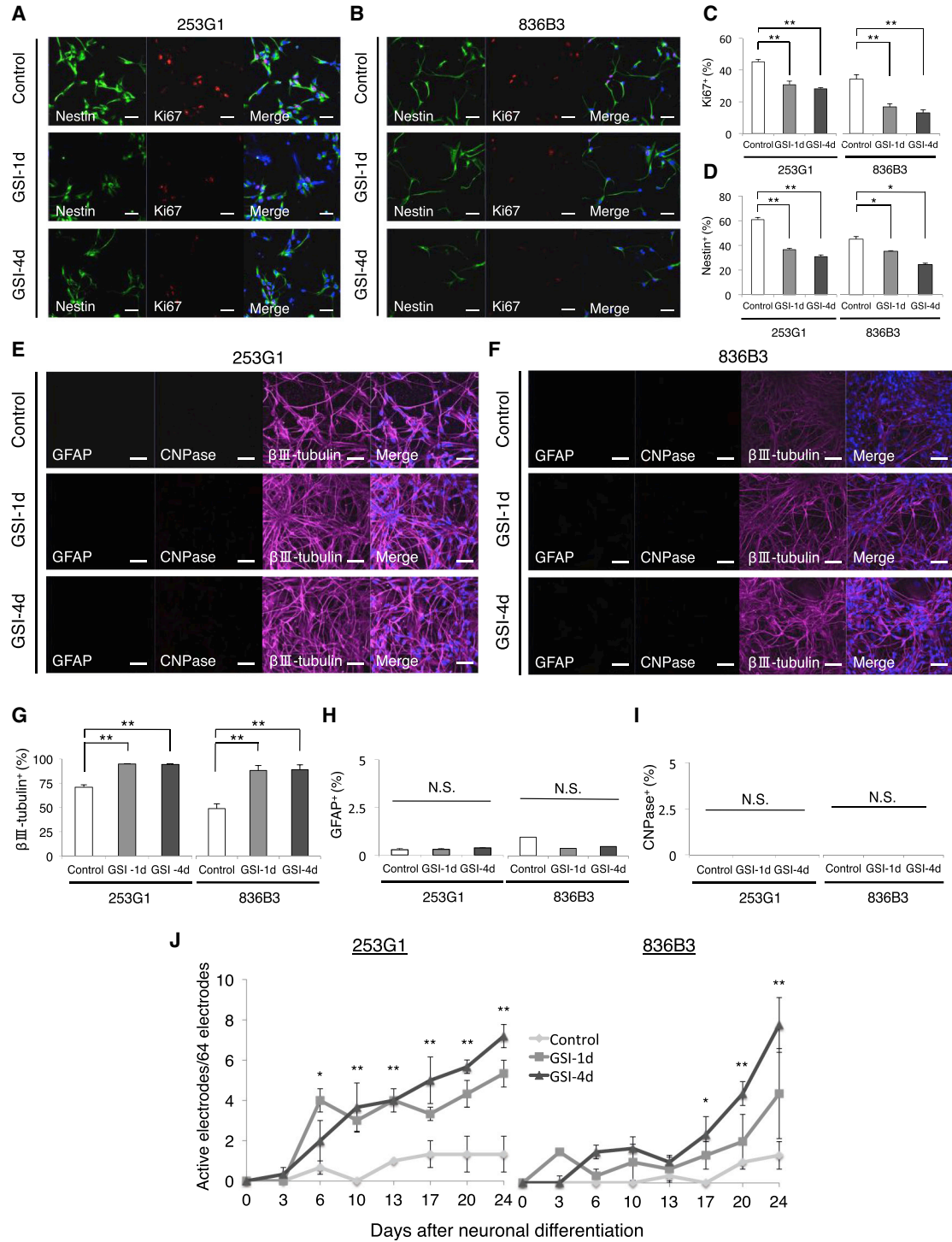
Figure 2. Neuronal Differentiation and Neuronal Maturation of hiPSC-NS/PCs Treated with or without GSI

(A and B) hiPSC-NS/PCs (with or without GSI treatment) dissociated into single cells, seeded on coverglasses, and immunostained for Ki-67 (cell proliferation marker) and Nestin (a neural stem cell marker). The nuclei were stained with Hoechst 33258. The micrographs show representative staining results for each group. Scale bars, 50 μm.

(C and D) Histograms showing the percentage of Ki-67$^+$ and Nestin$^+$ cells (n = 5 independent experiments).

(legend continued on next page)

overgrowth of the graft-derived cells. A previous study by our group showed that 253G1 hiPSC-NS/PCs are characterized by tumor-like overgrowth following cell transplantation in the injured spinal cord of NOD/SCID mice (Nori et al., 2015). In fact, 253G1 hiPSC-NS/PCs tended to grow and spread at a faster rate than 836B3 hiPSC-NS/PC transplants (our unpublished data). Here, we found that inhibiting Notch signaling with the GSI promoted the neuronal differentiation and maturation of hiPSC-NS/PCs in vitro, irrespective of the culture period and the cell line (Figure 2). Thus, we pretreated the 253G1 hiPSC-NS/PCs with the GSI for 1 day before cell transplantation. To monitor the survival and growth of the transplanted cells in the mouse injured spinal cord, we lentivirally transduced the hiPSC-NS/PCs with ffLuc, a fusion protein between a fluorescent protein Venus and a firefly luciferase (Hara-Miyauchi et al., 2012), which allowed us to identify the transplanted cells by their bioluminescent luciferase signals and fluorescent Venus signals. The photon counts and the number of the hiPSC-NS/PCs were significantly correlated (r^2 = 0.998, Figures S3A–S3C). The photon counts of the transplanted hiPSC-NS/PCs decreased within the first 7 days, although they gradually increased at 14 days after cell transplantation. In the control group, the photon counts were prominently increased compared with that of the GSI$^+$ group between 28 and 89 days after cell transplantation (Figures 4A and 4B). The photon counts of the control group increased more than 10-fold from their initial values at 89 days after cell transplantation. In the GSI$^+$ group, the photon counts increased more slowly and reached a plateau at 28 days after cell transplantation. Representative results of H&E staining of spinal cords from the control group and the GSI$^+$ group after injury and transplantation are shown in Figure 4C. In the control group, the HNA$^+$ transplanted cells occupied the entire spinal cord, whereas the cells in the GSI$^+$ group did not. The volumes and sizes of the grafts that were pretreated with GSI were significantly smaller than the grafts in the control group (volume of grafts: control group 7.3 ± 1.5 mm^2, GSI$^+$ group 1.3 ± 0.6 mm^2; Figures 4D and 4E). After transplantation into the injured spinal cord, the transplanted hiPSC-NS/PCs differentiated into three neural lineages in each group, such as pan-ELAVL (Hu)$^+$ neurons, GFAP$^+$ astrocytes, and APC$^+$ oligodendrocytes.

We also detected the Ki-67$^+$ and Nestin$^+$ cells (Figure 4F). Immunostaining for various cell markers was examined 89 days after transplantation and subjected to quantitative analyses to evaluate the differentiation phenotype of the transplanted cells in vivo. The proportion of pan-ELAVL (Hu)$^+$ cells was significantly increased (control group 15.6% ± 1.2%, GSI$^+$ group 51.0% ± 1.8%) in the GSI$^+$ group, although the proportion of Ki-67$^+$ cells (control group 17.9$^+$ ± 0.9%, GSI$^+$ group 3.9% ± 0.9%) and that of Nestin$^+$ cells (control group 30.3% ± 1.6%, GSI$^+$ group 5.3% ± 0.8%) were also significantly decreased compared with the control group. The proportion of GFAP$^+$ cells (control group 15.6% ± 1.1%, GSI$^+$ group 11.5% ± 3.9%) and that of APC$^+$ cells (control group 5.2$^+$ ± 1.1%, GSI$^+$ group 4.2% ± 1.0%) were not significantly different between the control group and the GSI$^+$ group (Figure 4G).

We examined triple immunostaining with HNA, βIII-tubulin, and mouse-specific Bassoon (Bsn), a presynaptic marker, to evaluate the ability of the GSI-pretreated transplanted cell-derived neurons to integrate with host neural circuitry. βIII-tubulin$^+$/HNA$^+$ cells that were transplanted in parenchymal locations were contacted by Bsn$^+$ synaptic boutons of the host neurons (Figure S4A). Moreover, triple immunostaining for HNA, βIII-tubulin, and human-specific synaptophysin (hSyn) revealed that hSyn$^+$ boutons apposed the host mouse neurons (βIII-tubulin$^+$/HNA$^-$) (Figure S4B). Furthermore, immunostaining for Notch1, activated Notch1, and Snail were examined 89 days after transplantation and subjected to quantitative analyses to confirm the level of Notch activation and EMT in the transplanted cells in vivo. In the GSI$^+$ group, the proportion of Notch1$^+$ cells (control group 43.1% ± 7.2%, GSI$^+$ group 2.5% ± 2.3%), activated Notch1$^+$ cells (control group 34.1% ± 3.2%, GSI$^+$ group 0.55% ± 0.35%), and Snail$^+$ cells (control group 36.7% ± 5.1%, GSI$^+$ group 0%) were all significantly decreased compared with that of the control group (Figures 5A–5F).

Transplantation of Tumorigenesis-/Overgrowth-Prone hiPSC-NS/PCs Pretreated with GSI Maintains Motor Functional Recovery after SCI

We evaluated locomotor function using the Basso Mouse Scale (BMS) score, rotarod testing, and treadmill gait analyses with the DigiGait system. In the control group, the

---

(E and F) Fourteen days after neuronal induction, the hiPSC-NS/PCs were immunostained for βIII-tubulin (a neuron marker), GFAP (an astrocyte marker), and CNPase (an oligodendrocyte marker). The nuclei were stained with Hoechst 33258. The micrographs show representative staining results for each group. Scale bars, 50 μm.

(G–I) Histograms showing the percentage of βIII-tubulin$^+$, GFAP$^+$, and CNPase$^+$ cells (n = 5 independent experiments).

(J) Daily analyses of neuronal maturation using MEA, which measures the active electrodes in each group (n = 5 independent experiments).

$*p < 0.05$, $**p < 0.01$, and not significant (N.S.) according to one-way ANOVA with the Tukey-Kramer test. Data are presented as means ± SEM.
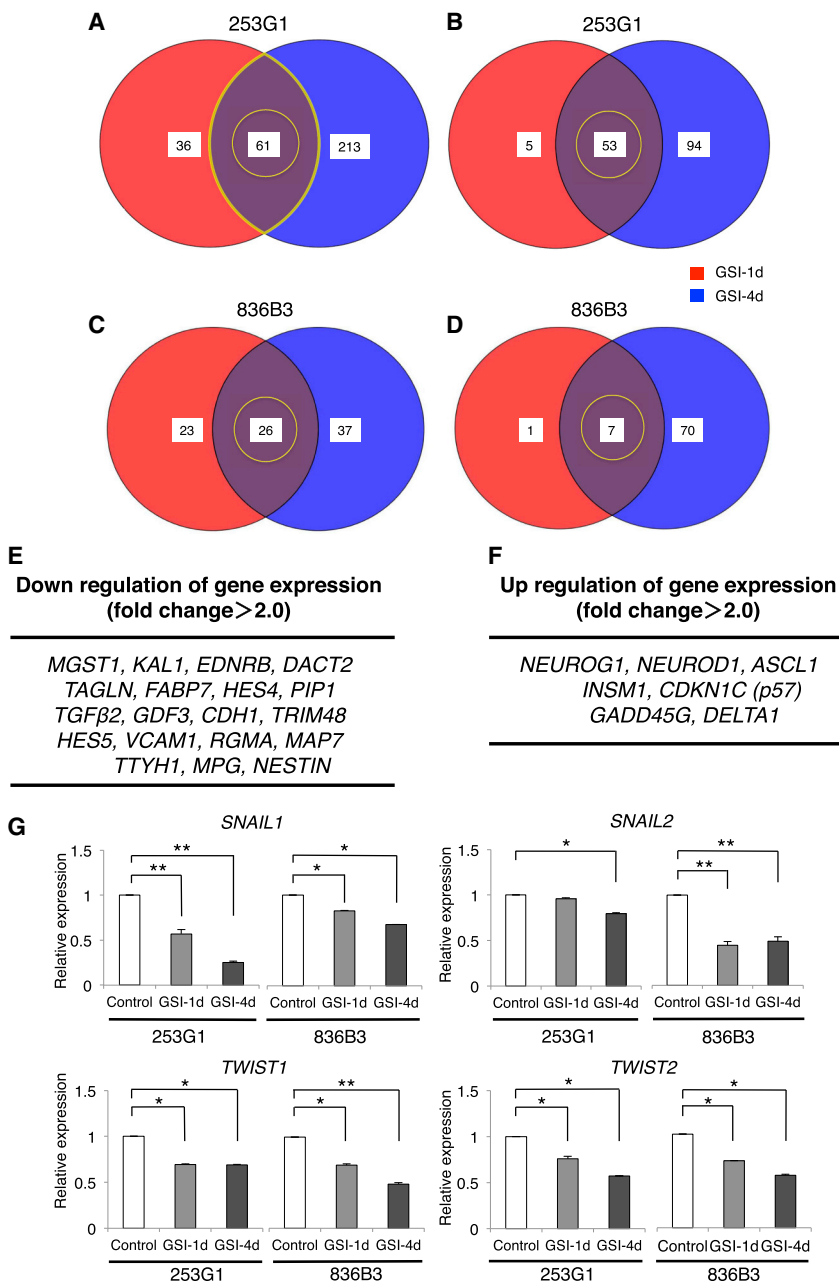
Figure 3. DNA Microarray and RT-PCR Analyses of GSI-Treated hiPSC-NS/PCs

(A) Venn diagrams showing the human genes with decreased expression in each group of GSI-treated 253G1 hiPSC-NS/PCs. Color key: red, 36 genes with decreased expression in the GSI-1d group; blue, 213 genes with decreased expression in the GSI-4d group; purple, 61 genes with decreased expression in both groups (n = 3 independent experiments).

(B) Venn diagrams showing the human genes with increased expression in each group of GSI-treated 253G1 hiPSC-NS/PCs. Color key: red, 5 genes with increased expression in the GSI-1d group; blue, 94 genes with increased expression in the GSI-4d group; purple, 53 genes with increased expression in both groups (n = 3 independent experiments).

(C) Venn diagrams showing the human genes with decreased expression in the GSI-1d and GSI-4d group of 836B3 hiPSC-NS/PCs. Color key: red, 23 genes with decreased expression in the GSI-1d group; blue, 37 genes with decreased expression in the GSI-4d group; purple, 26 genes with decreased expression in both groups (n = 3 independent experiments).

(D) Venn diagrams showing the human genes with increased expression in the GSI-1d and GSI-4d groups of 836B3 hiPSC-NS/PCs. Color key: red, 1 gene with increased expression in the GSI-1d group; blue, 70 genes with increased expression in the GSI-4d group; purple, 7 genes with increased expression in both groups (n = 3 independent experiments).

(E and F) (E) Lists showing the downregulated and (F) upregulated genes compared with control and GSI-1d and GSI-4d groups for each cell line using DNA microarrays (fold change >2.0).

(G) qRT-PCR analyses of known EMT-related genes in the GSI-1d and GSI-4d groups compared with the control group (equal to 1). The data were normalized to the reference *GAPDH* levels (n = 3 independent experiments). *p < 0.05 and **p < 0.01 according to one-way ANOVA with the Tukey-Kramer test. Data are presented as means ± SEM.

See also Figure S1.

recovery of motor function persisted for up to 35 days after transplantation, although thereafter hindlimb motor function exhibited gradual deterioration according to the BMS score. In the GSI+ group, significantly greater functional recovery was observed relative to the PBS group and the control group at 42 days after transplantation and was maintained thereafter (Figure 6A). The gait performance of the mice in each group was analyzed us-

ing the rotarod test and the DigiGait system at 89 days after transplantation. In the GSI+ group, the mice remained on the rotating rod for a significantly longer time than the mice in the PBS group and the control group (Figure 6B), and all of the mice could sufficiently walk on a treadmill at 7 cm/s to perform the test. The gait analyses also revealed a significantly longer stride length in the GSI+ group than in the PBS and control groups (Figure 6C).

Transplantation of Normal/Safe hiPSC-NS/PCs Pretreated with GSI Survive and Enhance Motor Functional Recovery Following SCI

Finally, we elucidated the long-term effects of GSI pretreatment on normal/safe hiPSC-NS/PCs that were transplanted into SCI model mice. Our group previously showed that 201B7 hiPSC-NS/PCs are "normal/safe" cell lines that did not display tumor-like overgrowth following transplantation in the injured spinal cord of NOD/SCID mice (Nori et al., 2011, 2015). We transplanted 201B7 hiPSC-NS/PCs with and without GSI treatment and examined their behavior after transplantation. The photon counts reached a plateau at 14 days after cell transplantation in each group (Figures 7A and 7B). The volume and size of the grafts were not significantly different between the control group and the GSI$^+$ group (graft volume: control group 2.2 ± 0.5 mm^2, GSI$^+$ group 2.1 ± 0.5 mm^2; Figures 7C–7E). In each group, the transplanted hiPSC-NS/PCs survived and did not cause tumor-like overgrowth. We examined the effects of transplantation for hiPSC-NS/PCs with and without GSI treatment on axonal regrowth after SCI by immunostaining analyses. More neurofilament 200-kDa-positive neuronal fibers and 5-hydroxytryptamine-positive serotonergic fibers were observed in the GSI$^+$ group than in the PBS and control groups (Figures S5A and S5B). In the GSI$^+$ group, there were also significantly more growth-associated protein 43-positive fibers in the ventral region 1 mm caudal to the lesion epicenter than in the PBS and control groups (Figures S5C and S5D).

The recovery of motor function persisted for up to 89 days after transplantation in each group compared with the PBS group. Furthermore, in the GSI$^+$ group, significantly greater functional recovery occurred compared with the control group at 35 days after transplantation (Figure 7F). In the GSI$^+$ group, the mice remained on the rotating rod for a significantly longer time those in the PBS and control groups (Figure 7G). In the treadmill gait analyses, significant differences were not observed in stride length between the control group and the GSI$^+$ group (Figure 7H).

DISCUSSION

In the present study, we report seven major findings. First, after the hiPSC-NS/PCs were treated with the GSI, the number of cells, the size of neurospheres, the proportion of cells in the S phase of the cell cycle, and the number of Ki-67$^+$ and Nestin$^+$ cells determined by immunostaining were all significantly decreased compared with that of the control group. Second, the proportion of βIII-tubulin$^+$ neuronal cells was significantly increased in the GSI-treated group compared with the control (Figure 1), and an MEA assay showed that the average number of active electrodes occurred significantly earlier and exhibited much more neuronal activity than the control group (Figure 2J). Third, the gene expression profiles of the GSI-treated hiPSC-NS/PCs obtained from the DNA microarray and RT-PCR showed that the expression of cell-cycle-related genes, mature neuronal marker-related genes, and p53-dependent genes was increased compared with that of the control group, which is consistent with decreases in pluripotency and self-renewal marker genes (Figure 3). Fourth, after transplantation of the hiPSC-NS/PCs in animal models of SCI, the photon counts of the transplanted cells increased more slowly and reached a plateau at 28 days in the GSI$^+$ groups as determined by bioluminescence (BLI) (Figures 4A and 4B). Fifth, in the GSI$^+$ group, the proportion of pan-ELAVL (Hu)$^+$ cells was significantly increased, although the proportion of Ki-67$^+$ cells, Nestin$^+$ cells, Notch1$^+$ cells, activated Notch1$^+$ cells, and Snail$^+$ cells was significantly decreased compared with that of the control group (Figures 4 and 5). Sixth, in the long-term observations, the control group showed deteriorated motor function accompanied by tumor-like overgrowth. However, the GSI$^+$ group maintained functional recovery and reduced the overgrowth of transplanted cells by inhibiting cell proliferation (Figure 6). Seventh, after transplantation of a normal/safe cell line, the grafts that were pretreated with GSI also survived and did not show tumor-like overgrowth, which caused motor functional recovery after SCI (Figure 7). Taken together, these results suggest that the GSI treatment induces the differentiation of hiPSC-NS/PCs into a more mature state with limited proliferation and contributes to functional recovery without tumor-like overgrowth in the injured spinal cord. We believe that this strategy improves the safety of hiPSC-NS/PC transplantation therapy for SCI.

Previous studies have reported that Notch signaling controls the induction of neural stem cells in vitro and in vivo during differentiation (Crawford and Roelink, 2007; Nelson et al., 2007). As established by Ogura et al. (2013), inhibition of this signaling pathway promotes the neuronal differentiation of neural progenitor cells derived from human iPSCs. Our in vitro experiments confirmed that by inhibiting Notch signaling with the GSI, a greater number of NS/PCs derived from two lines of human iPSCs with tumorigenesis-/overgrowth-prone characters (253G1 and 836B3) are induced to undergo neuronal differentiation and maturation, although they present limited proliferation.

Nelson et al. (2007) showed treatments with a GSI (DAPT) lasting at least 6 hr commits NS/PCs to neuronal differentiation, although *HES5* expression is reduced after 3 hr. In the present study, significant differences were not
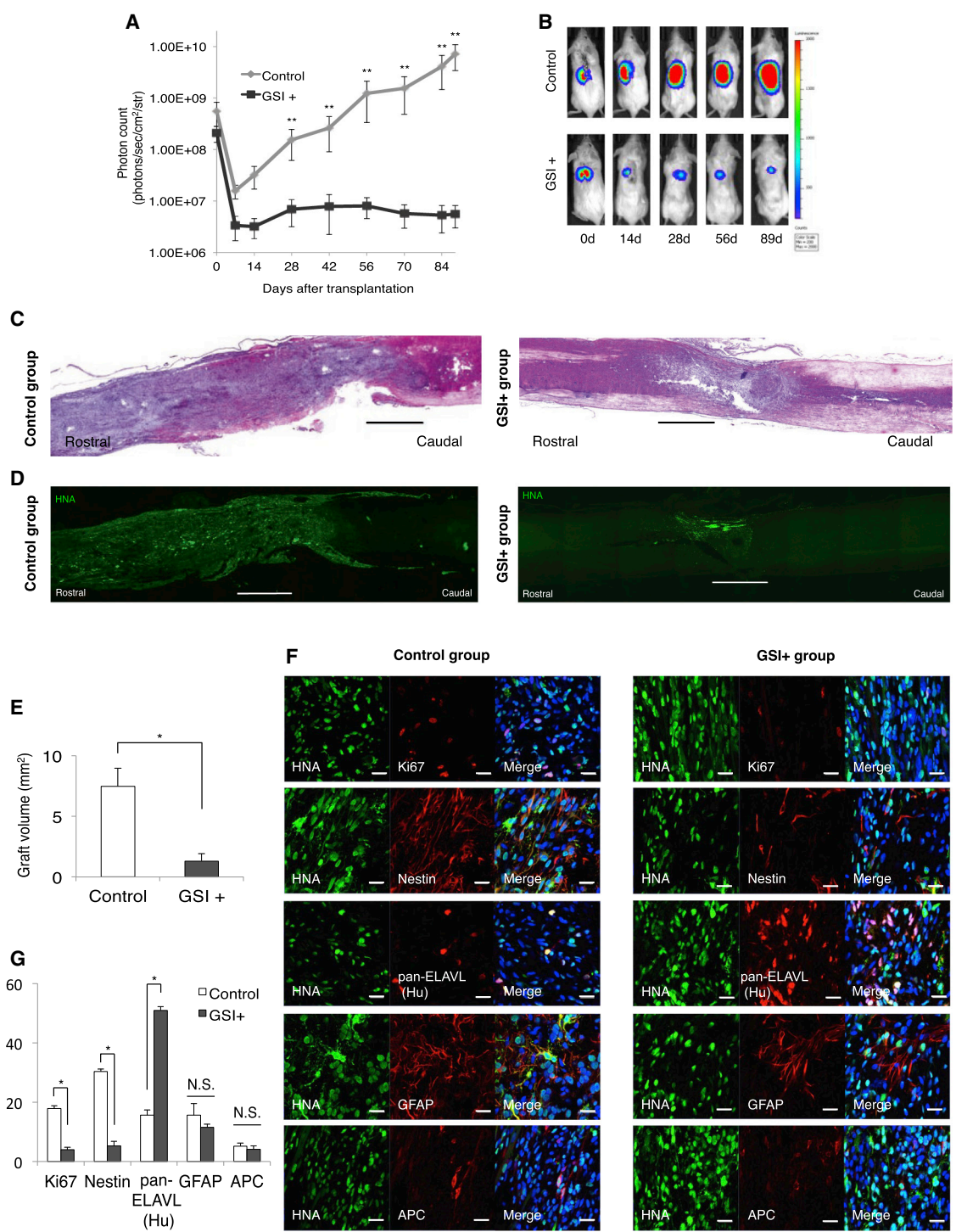
Figure 4. Long-Term Observation after Transplantation of GSI-Pretreated 253G1 hiPSC-NS/PCs

(A) Quantitative analyses of the photon counts derived from the transplanted cells until 89 days post transplantation (control group, n = 10 mice; GSI+ group, n = 10 mice).

(B) Representative images of mice at 0, 14, 28, 56, and 89 days after transplantation of 253G1 hiPSC-NS/PCs that were pretreated with or without GSI.

(C) Representative H&E-stained images of the spinal cord from each group at 89 days after transplantation. Scale bars, 1,000 μm.

(legend continued on next page)

A–C images with labels: HNA, Notch1, Merge; Control group and GSI+ group
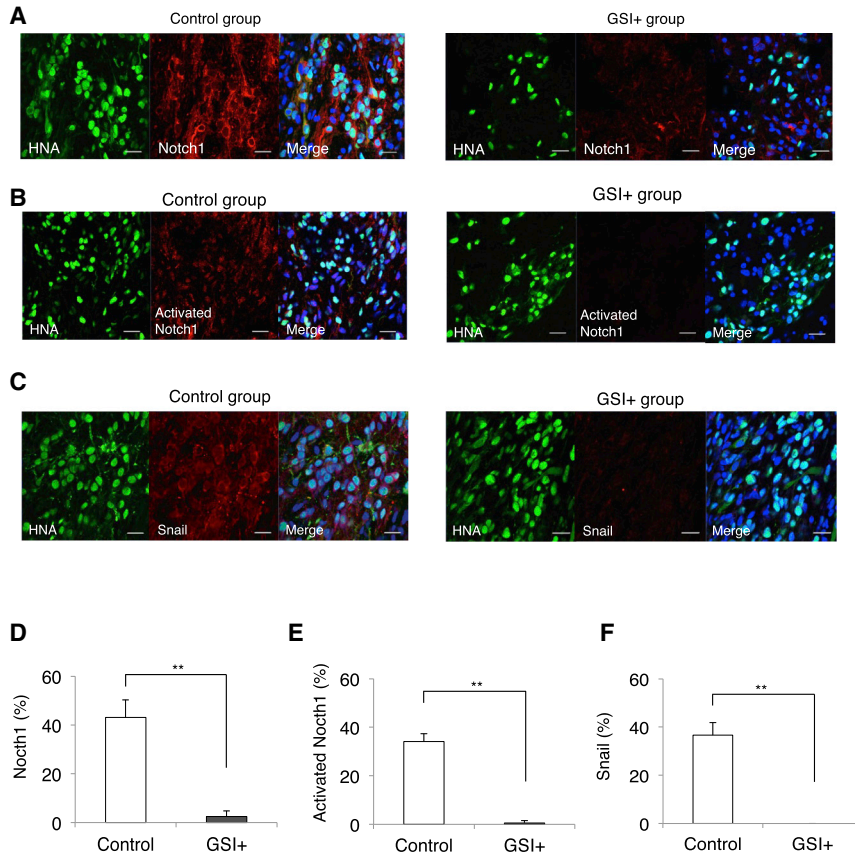
Figure 5. Level of Notch and EMT Activation in the Transplanted Cells Following Long-Term Observations In Vivo

(A–C) Representative images of immunohistochemical staining show the results for each group. The HNA^{+} transplanted cells were stained with Notch1, activated Notch1, and Snail. Scale bars, 20 μm.

(D–F) Histograms showing the percentages of cell-type-specific, marker-positive cells among the HNA^{+} transplanted cells at 89 days after transplantation (control group, n = 10 mice; GSI[+] group, n = 10 mice). **p < 0.01 according to the Wilcoxon rank-sum test. Data are presented as means ± SEM.

observed between the GSI-1d and GSI-4d group in hiPSC-NS/PC proliferation and differentiation, suggesting that inhibition of Notch signaling with a GSI promotes the neuronal differentiation and maturation of hiPSC-NS/PCs regardless of the culture period or cell lines.

Nori et al. (2011) showed that the 201B7 hiPSC-NS/PC-transplanted group exhibited significantly better functional recovery than the PBS-injected group more than 21 days after SCI as measured by the BMS score. In this study, the GSI[+] group of 253G1 hiPSC-NS/PC transplants ("bad" clone) exhibited confirmed functional recovery more than 21 days after SCI (BMS score: PBS group 2.5 ± 0.3 at 12 days post transplantation and 3.0 ± 0.1 at

89 days post transplantation; GSI[+] group 3.8 ± 0.7 at 12 days post transplantation and 4.8 ± 0.4 at 89 days post transplantation). Borghese et al. (2010) showed that the neural stem cell derived from human embryonic cells pretreated with DAPT were strongly positive for human synaptophysin, and exhibited strong human doublecortin staining compared with untreated cells after transplantation. In this study, the GSI[+] group of 201B7 hiPSC-NS/PC transplants ("good" clone) exhibited a significantly greater tendency to enhance the axonal regrowth in the mouse injured spinal cord, which are likely to have resulted in improved motor function compared with the control group at 26 days after transplantation. The improved

(D) Representative immunohistological images of HNA^{+} cells showing a graft from each group at 89 days after transplantation. Scale bars, 1,000 μm.

(E) Graft volumes of hiPSC-NS/PCs were measured and estimated for each group of SCI at 89 days after transplantation (control group, n = 10 mice; GSI[+] group, n = 10 mice).

(F) Representative images of the immunohistochemical staining show the results for each group. The HNA^{+} transplanted cells were stained with Ki-67, Nestin, pan-ELAVL (Hu), GFAP, and APC. Scale bar, 20 μm.

(G) Percentages of cell-type-specific, marker-positive cells among the HNA^{+} transplanted cells at 89 days after transplantation (control group, n = 10 mice; GSI[+] group, n = 10 mice).

*p < 0.05, **p < 0.01, and not significant (N.S.) according to one-way ANOVA with the Tukey-Kramer test (G) or Wilcoxon rank-sum test (A and E). Data are presented as means ± SEM.
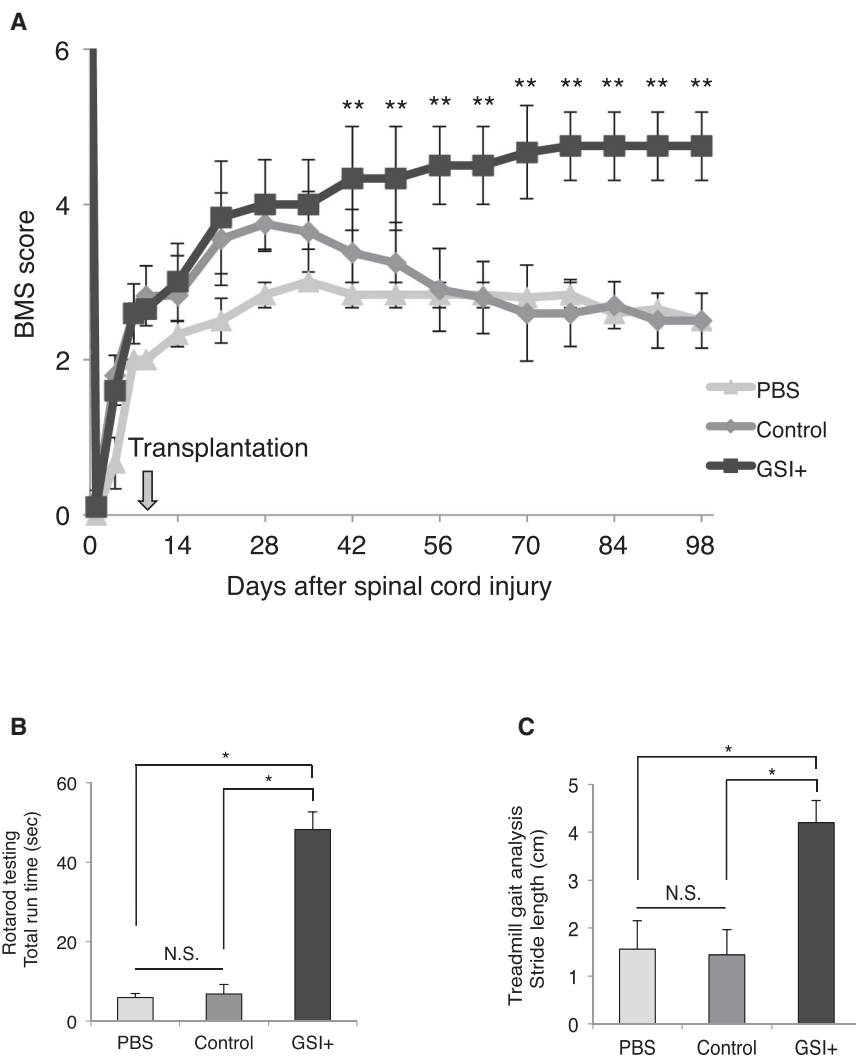
Figure 6. Long-Term Motor Function Analyses after Transplantation of GSI-Pretreated hiPSC-NS/PCs

(A) Comparison of the BMS scores among the PBS, control, and GSI+ groups. Motor function in the hind limbs was assessed weekly for up to 89 days after transplantation using the BMS score (PBS group, n = 10; control group, n = 10; GSI+ group, n = 10 mice).

(B) Comparison of the rotarod test among the PBS, control, and GSI+ groups. The rotarod test was performed at 89 days after transplantation. Histograms show the total run time (PBS group, n = 10; control group, n = 10; GSI+ group, n = 10 mice).

(C) Comparison of the stride lengths among the PBS, control, and GSI+ groups. Treadmill gait analyses were performed at 89 days after transplantation using the DigiGait system. Histograms show the stride length (PBS group, n = 10; control group, n = 10; GSI+ group, n = 10 mice).

$*p < 0.05$, $**p < 0.01$, and not significant (N.S.) according to two-way repeated-measures ANOVA with the Tukey-Kramer test (A) or one-way ANOVA with the Tukey-Kramer test (B and C). Data are presented as means ± SEM.

motor function was maintained after this point in the GSI+ group (BMS score: control group 3.8 ± 0.2 at 26 days post transplantation and 4.4 ± 0.5 at 89 days post transplantation; GSI+ group 4.3 ± 0.5 at 26 days post transplantation and 4.9 ± 0.3 at 89 days post transplantation). It is possible that pretreatment with GSI might have other mechanisms besides axonal regrowth, and could have a clinically meaningful effect and improve human iPSC-based transplantation for SCI.

Improved cell quality and safety, particularly with respect to the risk of tumor-like overgrowth, will be crucially important for any clinical use of hiPSC-NS/PCs. Okada et al. (2005) revealed that the photon counts measured by BLI analyses were significantly proportional to the number of the transplanted cells in vivo. Nori et al. (2015) indicated that some mice transplanted with 253G1 hiPSC-NS/PCs showed temporary motor function recovery for up to 47 days after transplantation; however,

the photon counts of the transplanted cells increased more than 10-fold from its initial value, and these mice also developed tumor-like overgrowth and deterioration of motor function at 103 days after transplantation. Therefore, the photon counts measured by BLI analyses could be useful for the diagnosis for detecting tumor-like overgrowth in the mouse injured spinal cords. In the present study, the control group (i.e., the group without GSI pretreatment) showed a rapid increase in the photon count of the transplanted cells and improvements in hindlimb motor function, which subsequently deteriorated gradually upon long-term observations. However, in the GSI+ groups, the photon counts increased more slowly and reached a plateau after transplantation. Greater functional recovery was also observed, and was maintained at significantly higher levels compared with the control group. In addition, we previously reported that the size of the tumors formed by the transplanted hiPSC-NS/PCs in the injured

spinal cord correlated with the proportion of Nestin$^+$ cells in the graft (Nori et al., 2015). The proportion of transplanted Nestin$^+$ cells decreased from 10.7% ± 2.2% at 47 days to 7.5% ± 1.0% at 103 days after transplanting 201B7 hiPSC-NS/PCs, resulting in no tumor-like overgrowth. The proportion of Nestin$^+$ cells increased from 19.6% ± 0.5% at 47 days to 33.1% ± 7.4% at 103 days after transplanting 253G1 hiPSC-NS/PCs. Therefore, we suggest that differentiation-resistant Nestin$^+$ cells proliferated over time and formed tumors. However, the present study showed that the proportion of transplanted Nestin$^+$ cells in the control group increased to 30.3% ± 1.6% at 89 days after transplantation and resulted in tumor-like overgrowth, whereas the proportion of Nestin$^+$ cells in the GSI$^+$ group decreased to 5.3% ± 0.8% at 89 days after transplantation and did not show evidence of tumor-like overgrowth. The proportion of Ki-67$^+$ cells in the control group was significantly increased to 17.9% ± 0.9% at 89 days after transplantation compared with the GSI$^+$ group. Furthermore, the proportion of pan-ELAVL (Hu)$^+$ neuronal cells in the GSI$^+$ groups significantly increased to 51.0% ± 1.8% compared with the control group at 89 days after transplantation, although significant differences were not observed in glial differentiation. Most of the GSI-pretreated, transplanted βIII-tubulin$^+$/HNA$^+$ cell-derived neurons were co-localized with Bsn$^+$ synaptic boutons of the host neurons, and hSyn$^+$ boutons were apposed to βIII-tubulin$^+$/HNA$^-$ host mouse neurons. These findings indicate that the proportion of proliferating/undifferentiating cells increases over time and induces tumor-like overgrowth in the vertebral canal of the mice. Therefore, the motor functional recovery observed in the control group subsequently deteriorated gradually upon long-term observations. However, pretreatment with GSI differentiated nearly all of these cells into mature neurons, which were further integrated into the reconstructed host neuronal network, where they formed synapses and prevented tumor-like overgrowth, even in mice transplanted with the "bad" clone, after observations for long periods. Therefore, significantly greater motor functional recovery was maintained compared with the control group.

The activation of Notch1 has been found to contribute to the invasion and metastasis of cancer via the EMT. In addition, Saad et al. (2010) showed that the overexpression of *NOTCH1* induces the expression of *SNAIL*. In the present study, after GSI treatment the expression of *NOTCH1*, *SNAIL1*, and *SNAIL2* was downregulated in vitro compared with the control group. Furthermore, the proportion of Notch1$^+$, activated Notch1$^+$, and Snail$^+$ cells was also significantly decreased after transplantation compared with the control group, which indicated that the presence of activated Notch1 on the transplanted cells reflected the γ-secretase-dependent activation of Notch1 in vivo. There-

fore, the GSI pretreatment could reduce the acquisition of EMT and inhibit the activation of Notch1 and Snail, which induced the transplanted cells to undergo neuronal maturation without tumor-like overgrowth upon transplantation of hiPSC-NS/PCs for SCI. However, Kopan and Ilagan (2004) showed that other signaling molecules act as targets for GSI. Thus, we cannot rule out the possibility that the GSI-induced inhibition of other signaling pathways, such as the expression of EMT-related genes, contributed to these results.

Longer differentiation periods have been shown to decrease the incidence of tumors. Alternatively, the selection of more mature cells using fluorescence-activated or magnetic-activated cell sorting, introduction of suicide genes, and irradiation of cells before transplantation may also help inhibit tumor-like overgrowth. However, these methods require long periods and more expensive processes to prepare the donor cells. In contrast, GSI pretreatment is a simple and inexpensive method that could be useful for improving the safety of hiPSC-NS/PCs transplantation therapy in SCI.

In conclusion, we confirmed that the GSI-treated hiPSC-NS/PCs exhibited a reduced proportion of dividing cells and increased neuronal maturation in vitro, and prevented the tumor-like overgrowth of transplanted cells by inhibiting cell proliferation, thereby resulting in safe and long-lasting functional recovery in vivo. Pretreatment of hiPSC-NS/PCs with GSI can improve the safety of hiPSC-NS/PC transplantation therapy for SCI.
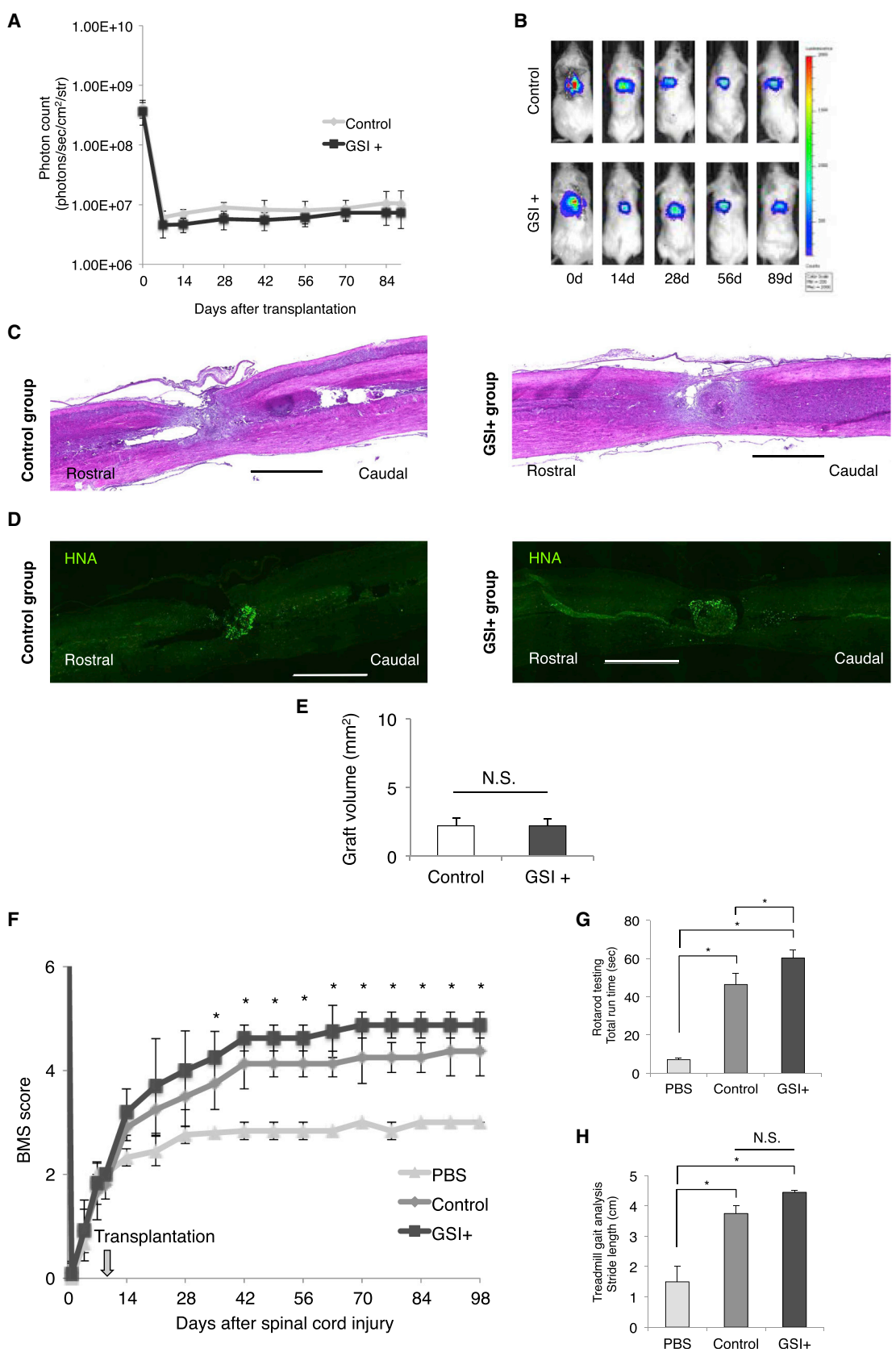
EXPERIMENTAL PROCEDURES

Cell Culture, hiPSC-NS/PC-Derived NS/PC Formation Assay, Neuronal Differentiation Analyses, and Lentiviral Transduction

The cell culture, hiPSC-NS/PC-derived NC/PC formation assay, neuronal differentiation analyses of several human iPSCs, and lentiviral transduction of neurospheres were performed as previously described (Nori et al., 2011, 2015; Okada et al., 2008). In brief, three hiPSC-NS/PCs lines were dissociated and infected with a lentivirus expressing ffLuc, a firefly luciferase fusion protein under the control of the EF promoter, to enable the detection of transplanted cells through their strong bioluminescent ffLuc signals in live SCI mice and in fixed spinal cord sections. Detailed methods are described in Supplemental Experimental Procedures.

Treatment of hiPSC-NS/PCs with GSI

One of the small-molecule GSIs, N-[N-(3,5-difluorophenacetyl)-l-alanyl]-S-phenylglycine t-butyl ester (DAPT; Sigma-Aldrich), is a potent nontransition-state analog inhibitor of γ-secretase that is thought to interact with the same active site between presenilin-1 heterodimers in γ-secretase complexes. DAPT was dissolved in DMSO at a final concentration of 10 μM. The highest

A

Photon count (photons/sec/cm²/str)

Days after transplantation

B

Control

GSI +

0d 14d 28d 56d 89d

C

Control group — Rostral / Caudal

GSI+ group — Rostral / Caudal

D

Control group — HNA — Rostral / Caudal

GSI+ group — HNA — Rostral / Caudal

E

Graft volume (mm²)

N.S.

Control   GSI +

F

BMS score

Days after spinal cord injury

Transplantation

PBS
Control
GSI+

G

Rotarod testing Total run time (sec)

PBS   Control   GSI+

H

Treadmill gait analysis Stride length (cm)

N.S.

PBS   Control   GSI+

(legend on next page)

concentration of this molecule that effectively inhibited the division of hiPSC-NS/PCs without precipitating in culture medium or producing toxic effects was determined in preliminary experiments. The hiPSC-NS/PCs were cultured in vitro with GSI for 1 day in the GSI-1d group, 4 days in the GSI-4d group, and without GSI in the control group. For the neuronal differentiation, proliferation, and cell transplantation assays, the hiPSC-NS/PCs were used after the fifth passage.

Flow Cytometric Analyses

In the cell-cycle analyses, the hiPSC-NS/PCs were dissociated into single cells and double immunofluorescence staining was performed with the Click-iT Plus EdU Flow Cytometry Assay Kit (Life Technologies). In the apoptosis analyses, double immunofluorescence staining was performed using the primary antibodies anti-allophycocyanin (APC)-labeled annexin V (561012) and 7-amino-actinomycin D (7-AAD, 559925) (BD Biosciences). The cells were stained with a mixture of these primary antibodies for 15 min at 37°C. Detailed methods are described in Supplemental Experimental Procedures.

Microelectrode Array

The MEA was performed as previously described (Köhling et al., 2005), and detailed methods are provided in Supplemental Experimental Procedures.

DNA Microarray Analyses

DNA microarray analyses were performed as previously described (Parinya et al., 2014), and detailed methods are provided in Supplemental Experimental Procedures. GO accessions are listed and shown in Tables S1 and S2.

qRT-PCR

RNA isolation and RT-PCR were performed as previously described (Nori et al., 2011, 2015; Okada et al., 2008), and detailed protocols are provided in Supplemental Experimental Procedures.

SCI Animal Model and hiPSC-NS/PC Transplantation

Contusive SCI was induced at the level of the tenth thoracic spinal vertebra in the spinal cords of adult female NOD-SCID mice. Nine days after SCI, hiPSC-NS/PCs that had been pretreated with or without GSI (5×10^5 cells/2 μL) were transplanted into the lesion epicenter of each mouse. All experiments were performed in accordance with the Guidelines for the Care and Use of Laboratory Animals of Keio University (Assurance No. 13020) and the NIH Guide for the Care and Use of Laboratory Animals. Detailed methods are provided in Supplemental Experimental Procedures.

Histological Analysis

Histological analyses were performed at 89 days after transplantation. Spinal cord sections were histologically evaluated by H&E staining and immunohistochemistry (IHC). Detailed protocols are provided in Supplemental Experimental Procedures.

Behavioral Analyses

The motor function of each mouse in the PBS group, the control group, and the GSI[+] group was evaluated weekly for up to 98 days after injury using the BMS scores (Basso et al., 2006). Detailed methods are provided in Supplemental Experimental Procedures.

Statistical Analysis

All data are reported as mean ± SEM. A Wilcoxon rank-sum test was used to evaluate the differences between groups with respect to the BLI analyses, H&E staining, and IHC results. One-way ANOVA followed by the Tukey-Kramer test for multiple comparisons was used to evaluate the differences in the following: number of living cells; sphere size; flow cytometric analyses of the cell cycle/apoptosis assays; neuronal differentiation analyses; MEA; DNA microarray analyses; RT-PCR gene expression profile analyses; and the rotarod and DigiGait results. Two-way repeated-measures ANOVA tests followed by the Tukey-Kramer test were used for the BMS analyses. p Values of <0.05 or <0.01 were considered to indicate statistical significance.

Figure 7. Long-Term Observations after Transplantation of GSI-Pretreated 201B7 hiPSC-NS/PCs

(A) Quantitative analyses of the photon counts derived from the transplanted cells until 89 days post transplantation (control group, n = 10 mice; GSI[+] group, n = 10 mice).

(B) Representative images of mice at 0, 14, 28, 56, and 89 days after transplantation of 201B7 hiPSC-NS/PCs that were pretreated with or without GSI.

(C) Representative H&E-stained images of the spinal cords from each group at 89 days after transplantation. Scale bars, 1,000 μm.

(D) Representative immunohistological images of HNA^{+} cells, showing a graft from each group at 89 days after transplantation. Scale bars, 1,000 μm.

(E) Graft volumes of the hiPSC-NS/PCs were measured and estimated for each group of SCI model animals at 89 days after transplantation (control group, n = 10 mice; GSI[+] group, n = 10 mice).

(F) Comparison of the BMS scores among the PBS, control, and GSI[+] groups. Motor function in the hind limbs was assessed weekly for up to 89 days after transplantation using the BMS score (PBS group, n = 10; control group, n = 10; GSI[+] group, n = 10 mice).

(G) Comparison of the rotarod test among the PBS, control, and GSI[+] groups. The rotarod test was performed at 89 days after transplantation. Histograms show the total run time (PBS group, n = 10; control group, n = 10; GSI[+] group, n = 10 mice).

(H) Comparison of the stride lengths among the PBS, control, and GSI[+] groups. Treadmill gait analyses were performed at 89 days after transplantation using the DigiGait system. Histograms show the stride lengths (PBS group, n = 10; control group, n = 10; GSI[+] group, n = 10 mice).

*p < 0.05 and not significant (N.S.) according to the Wilcoxon rank-sum test (A and E), two-way repeated-measures ANOVA with the Tukey-Kramer test (F), or one-way ANOVA with the Tukey-Kramer test (G and H). Data are presented as means ± SEM.

REFERENCES

Basso, D.M., Fisher, L.C., Anderson, A.J., Jakeman, L.B., McTigue, D.M., and Popovich, P.G. (2006). Basso Mouse Scale for locomotion detects differences in recovery after spinal cord injury in five common mouse strains. J. Neurotrauma 23, 635–659.

Borghese, L., Dolezalova, D., Opitz, T., Haupt, S., Leinhaas, A., Steinfarz, B., Koch, P., Edenhofer, F., Hampl, A., and Brüstle, O. (2010). Inhibition of Notch signaling in human embryonic stem cell-derived neural stem cells delays G1/S phase transition and accelerates neuronal differentiation in vitro and in vivo. Stem Cells 28, 955–964.

Crawford, T.Q., and Roelink, H. (2007). The notch response inhibitor DAPT enhances neuronal differentiation in embryonic stem cell-derived embryoid bodies independently of sonic hedgehog signaling. Dev. Dyn. 236, 886–892.

Cummings, B.J., Uchida, N., Tamaki, S.J., Salazar, D.L., Hooshmand, M., Summers, R., Gage, F.H., and Anderson, A.J. (2005). Human neural stem cells differentiate and promote locomotor recovery in spinal cord-injured mice. Proc. Natl. Acad. Sci. USA 102, 14069–14074.

Falk, A., Koch, P., Kesavan, J., Takashima, Y., Ladewig, J., Alexander, M., Wiskow, O., Tailor, J., Trotter, M., Pollard, S., et al. (2012). Capture of neuroepithelial-like stem cells from pluripotent stem cells provides a versatile system for in vitro production of human neurons. PLoS One 7, e29597.

Fujimoto, Y., Abematsu, M., Falk, A., Tsujimura, K., Sanosaka, T., Juliandi, B., Semi, K., Namihira, M., Komiya, S., Smith, A., et al. (2012). Treatment of a mouse model of spinal cord injury by transplantation of human induced pluripotent stem cell-derived long-term self-renewing neuroepithelial-like stem cells. Stem Cells 30, 1163–1173.

Hara-Miyauchi, C., Tsuji, O., Hanyu, A., Okada, S., Yasuda, A., Fukano, T., Akazawa, C., Nakamura, M., Imamura, T., Matsuzaki, Y., et al. (2012). Bioluminescent system for dynamic imaging of cell and animal behavior. Biochem. Biophys. Res. Commun. 419, 188–193.

Hofstetter, C.P., Holmström, N.A., Lilja, J.A., Schweinhardt, P., Hao, J., Spenger, C., Wiesenfeld-Hallin, Z., Kurpad, S.N., Frisén, J., and Olson, L. (2005). Allodynia limits the usefulness of intraspinal neural stem cell grafts; directed differentiation improves outcome. Nat. Neurosci. 8, 346–353.

Iwanami, A., Kaneko, S., Nakamura, M., Kanemura, Y., Mori, H., Kobayashi, S., Yamasaki, M., Momoshima, S., Ishii, H., Ando, K., et al. (2005). Transplantation of human neural stem cells for spinal cord injury in primates. J. Neurosci. Res. 80, 182–190.

Kobayashi, Y., Okada, Y., Itakura, G., Iwai, H., Nishimura, S., Yasuda, A., Nori, S., Hikishima, K., Konomi, T., Fujiyoshi, K., et al. (2012). Pre-evaluated safe human iPSC-derived neural stem cells promote functional recovery after spinal cord injury in common marmoset without tumorigenicity. PLoS One 7, e52787.

Kopan, R., and Ilagan, M.X. (2004). Gamma-secretase: proteasome of the membrane? Nat. Rev. Mol. Cell Biol. 5, 499–504.

Kumagai, G., Okada, Y., Yamane, J., Nagoshi, N., Kitamura, K., Mukaino, M., Tsuji, O., Fujiyoshi, K., Katoh, H., Okada, S., et al. (2009). Roles of ES cell-derived gliogenic neural stem/progenitor cells in functional recovery after spinal cord injury. PLoS One 4, e7706.

Köhling, R., Melani, R., Koch, U., Speckmann, E.J., Koudelka-Hep, M., Thiébaud, P., and Balestrino, M. (2005). Detection of electrophysiological indicators of neurotoxicity in human and rat brain slices by a three-dimensional microelectrode array. Altern. Lab. Anim. 33, 579–589.

Miura, K., Okada, Y., Aoi, T., Okada, A., Takahashi, K., Okita, K., Nakagawa, M., Koyanagi, M., Tanabe, K., Ohnuki, M., et al. (2009). Variation in the safety of induced pluripotent stem cell lines. Nat. Biotechnol. 27, 743–745.

Nelson, B.R., Hartman, B.H., Georgi, S.A., Lan, M.S., and Reh, T.A. (2007). Transient inactivation of Notch signaling synchronizes differentiation of neural progenitor cells. Dev. Biol. 304, 479–498.

Nori, S., Okada, Y., Yasuda, A., Tsuji, O., Takahashi, Y., Kobayashi, Y., Fujiyoshi, K., Koike, M., Uchiyama, Y., Ikeda, E., et al. (2011). Grafted human-induced pluripotent stem-cell-derived neurospheres promote motor functional recovery after spinal cord injury in mice. Proc. Natl. Acad. Sci. USA *108*, 16825–16830.

Nori, S., Okada, Y., Nishimura, S., Sasaki, T., Itakura, G., Kobayashi, Y., Francois, R.H., Shimizu, A., Koya, I., Yoshida, R., et al. (2015). Long-term safety issues of iPSC-based cell therapy in a spinal cord injury model: oncogenic transformation with epithelial-mesenchymal transition. Stem Cell Rep. *4*, 360–373.

Ogawa, Y., Sawamoto, K., Miyata, T., Miyao, S., Watanabe, M., Nakamura, M., Bregman, B.S., Koike, M., Uchiyama, Y., Toyama, Y., and Okano, H. (2002). Transplantation of in vitro-expanded fetal neural progenitor cells results in neurogenesis and functional recovery after spinal cord contusion injury in adult rats. J. Neurosci. Res. *69*, 925–933.

Ogura, A., Morizane, A., Nakajima, Y., Miyamoto, S., and Takahashi, J. (2013). γ-Secretase inhibitors prevent overgrowth of transplanted neural progenitors derived from human-induced pluripotent stem cells. Stem Cell Dev. *22*, 374–382.

Okada, Y., Shimazaki, T., Sobue, G., and Okano, H. (2004). Retinoic acid concentration dependent acquisition of neural cell identity during in vitro differentiation of mouse embryonic stem cells. Dev. Biol. *275*, 124–142.

Okada, S., Ishii, K., Yamane, J., Iwanami, A., Ikegami, T., Katoh, H., Iwamoto, Y., Nakamura, M., Miyoshi, H., Okano, H.J., et al. (2005). In vivo imaging of engrafted neural stem cells: its application in evaluating the optimal timing of transplantation for spinal cord injury. FASEB J. *19*, 1839–1841.

Okada, Y., Matsumoto, A., Shimazaki, T., Enoki, R., Koizumi, A., Ishii, S., Itoyama, Y., Sobue, G., and Okano, H. (2008). Spatiotemporal recapitulation of central nervous system development by murine embryonic stem cell-derived neural stem/progenitor cells. Stem Cells *26*, 3086–3098.

Okano, H., Nakamura, M., Yoshida, K., Okada, Y., Tsuji, O., Nori, S., Ikeda, E., Yamanaka, S., and Miura, K. (2013). Steps toward safe cell therapy using induced pluripotent stem cells. Circ. Res. *112*, 523–533.

Parinya, N., Carina, L., Kartiek, K., Riikka, L., Harri, L., Ritta, L., Karolina, L., Hataiwan, C., Timo, O., Tiom, T., et al. (2014). Notch signaling regulates the differentiation of neural crest from human pluripotent stem cells. J. Cell Sci. *127*, 2083–2094.

Saad, S., Stanners, S.R., Yong, R., Tang, O., and Pollock, C.A. (2010). Notch mediated epithelial to mesenchymal transformation is associated with increased expression of the Snail transcription factor. Int. J. Biochem. Cell Biol. *42*, 1115–1122.

Salazar, D.L., Uchida, N., Hamers, F.P., Cummings, B.J., and Anderson, A.J. (2010). Human neural stem cells differentiate and promote locomotor recovery in an early chronic spinal cord injury NOD-scid mouse model. PLoS One *5*, e12272.

Tsuji, O., Miura, K., Okada, Y., Fujiyoshi, K., Mukaino, M., Nagoshi, N., Kitamura, K., Kumagai, G., Nishino, M., Tomisato, S., et al. (2010). Therapeutic potential of appropriately evaluated safe-induced pluripotent stem cells for spinal cord injury. Proc. Natl. Acad. Sci. USA *107*, 12704–12709.

Yasuda, A., Tsuji, O., Shibata, S., Nori, S., Takano, M., Kobayashi, Y., Takahashi, Y., Fujiyoshi, K., Hara, C.M., Miyawaki, A., et al. (2011). Significance of remyelination by neural stem/progenitor cells transplanted into the injured spinal cord. Stem Cells *29*, 1983–1994.